

論文 / 著書情報
Article / Book Information

Title	New type sand compaction pile method for densification of liquefiable ground underneath existing structure
Authors	Masaki Kitazume, Akihiro Takahashi, Kenji Harada, Naotoshi Shinkawa
Citation	Journal of Geo-Engineering Sciences, Vol. 3, No. 1, pp. 1-13
Pub. date	2016, 6
Note	The final publication is available at IOS Press through http://dx.doi.org/10.3233/JGS-150032
Note	This file is author (final) version.

1 **New type sand compaction pile method for densification of liquefiable ground**
2 **underneath existing structure**

3
4 **Masaki Kitazume¹, Akihiko Takahashi¹, Kenji Harada² and Naotoshi Shinkawa²**

5 ¹ *Tokyo Institute of Technology, Tokyo, Japan*

6 ² *Fudo Tetra Corporation, Tokyo, Japan*

7
8 **Abstract**

9
10 The 2011 Great East Japan Earthquake caused severe damage to infrastructures due to
11 liquefaction, in which many embankments failed with large settlement and slope failure. Sand
12 Compaction Pile method is one of the typical ground improve- ment methods to densify the
13 ground by installing compacted sand piles into ground. This method has been often applied to
14 mitigate the liquefaction. However, current SCP method of constructing sand piles in vertical
15 direction is not able to densify ground underneath an existing structure. For applying the
16 method to an existing structure, a new type of SCP method was recently developed where in
17 compacted sand columns can be constructed in any direction. This paper briefly introduces
18 the new type of SCP method and the effectiveness of local densification by numerical
19 analysis. In this manuscript, a series of numerical analyses were conducted to evaluate the
20 effect of shape and location of SCP improved zone on the dynamic response of embankment.
21 This paper describes the numerical analyses as well as the development, machinery and
22 procedure of the technique, and emphasizes the uniqueness and effectiveness of the technique
23 for preventing liquefaction for new and existing structures.

24
25 **Keywords:** Sand Compaction Pile method, liquefaction, ground improvement, seismic
26 reinforcement, embankment, finite element analysis

27
28 **Journal of Geo-Engineering Sciences, 3(1), 1-13, 2016**

29 **Original URL:**

30 <http://dx.doi.org/10.3233/JGS-150032>

33 1. Introduction

34 In Japan, soft alluvial ground is frequently encountered on land and marine constructions. Sandy
35 soil has relatively preferable properties for compressibility, but liquefaction might happen
36 during earthquake in case of loose and saturated condition. In fact, many infrastructures were
37 heavily damaged in the 1995 Hyogoken-Nambu earthquake and the 2011 Tohoku earthquake
38 and tsunami. Many kinds of soil stabilization techniques were developed and available in
39 Japan for countermeasure for liquefaction. Among them, Sand Compaction Pile (SCP)
40 method has been developed in 1956 whose principal concept is to increase the ground density
41 by feeding a certain amount of granular material (usually sand) in the ground [1].
42 Effectiveness of the method as liquefaction countermeasure was firstly confirmed at the 1978
43 Miyagi-ken Oki earthquake in Japan and ever since the method has been often adopted for
44 many construction projects. In the construction procedure, a casing pipe is penetrated into a
45 ground vertically and during the withdrawal stage sand is fed into a ground through a casing
46 pipe and is compacted by vibration, dynamic impact or static excitation to construct a
47 compacted sand pile in the ground.

48 As infrastructures being developed in Japan, new technology is required to reinforce not
49 only new but also existing structures against anticipated huge earthquakes in future, where
50 ground underneath the structure should be compacted in the condition of limited working
51 space. Upon this, a quite unique sand compaction pile method, SAVE-SP method, was
52 developed in 2008 which enables to install sand piles vertically or at an angle in the ground [2].
53 In the method, granular sand is fluidized by mixing with special agent and water, and is
54 injected into ground through a small diameter pipe. The injected soil in the ground becomes
55 granular state by a slow-acting retarding plasticizer to create compacted sands. As the machine
56 for this method is small, it enables to construct at any direction underneath structure, which is
57 expected to prevent liquefaction more effectively. On the other hand, it encourages
58 establishing a new design procedure for precise evaluation of the improvement effect.

59 In this manuscript, a series of numerical analyses was conducted to evaluate the effect of
60 shape and location of SCP improved zone on the dynamic response of embankment. This
61 paper describes the numerical analyses as well as the development, machinery and procedure
62 of the technique, which emphasizes the uniqueness and effectiveness of the technique for
63 preventing liquefaction for new and existing structures.

64

65 2. Outline of new type sand compaction pile method

66

67 *2.1 Outline of the method*

68 Sand Compaction Pile (SCP) method was first developed in 1956 and has been frequently
69 applied to sandy ground and clay ground, where sand injected into a ground was compacted
70 by a vibrator installed on the top of casing pipe (vibratory SCP method). In order to minimize
71 adverse influence to surrounding caused by the vibrator, non-vibratory type SCP method was
72 developed in 1995 (Silent, Advanced Vibration-Erasing Composer, SAVE method), where
73 sand injected into a ground was statically compacted by the forced lifting/driving device
74 instead of the vibrator. In recent years, it is required to prevent liquefaction of ground
75 underneath existing structure such as building, river levee and airport runway. A sand
76 injection type SCP method (SAVE-SP method) was developed for the requirement as shown
77 in Fig. 1. In the method, granular sand is fluidized by mixing with special agent and water,
78 and is injected into ground through a small diameter pipe. The injected soil in the ground
79 becomes granular state by a slow-acting retarding plasticizer to create compacted sands, as
80 shown in Fig. 2. On the basis of the principle that this method depends on the operation to
81 inject sand into ground and to compact surrounding ground, the fluidized sand is required to
82 have antipodal properties of the fluidity by keeping water-retainability to avoid pipe clogging
83 and the modestly drainable characteristics to dissipate in order to obtain instantaneous high
84 density of sand when pumped into the ground. Also, slow-acting retarding plasticizer is added
85 to the fluidized sand to vanish the effect of fluidizing reagent after released into the ground.
86 Figure 3 compares the size of the three methods.

87 The characteristics of this method can be summarized as follow:

- 88 (1) The small-sized execution machine as shown in Fig. 3 enables to operate it at limited
89 working space and/or within a limited working time.
- 90 (2) The method is carried out through a small bore hole of about 10 cm in diameter, which
91 enables to minimize to influence to infrastructures in operation
- 92 (3) Sand pile is manufactured by static manner instead of dynamic, which provides negligible
93 vibration and noise influence to surrounding.
- 94 (4) The method is remarkably economic compared with conventional liquefaction
95 countermeasures available to work at small working space and/or for improvement

96 underneath existing structures.

97 (5) It is ecological and easily assimilates to the ground as natural sand is used.

98 ***2.2 Machine and execution***

99 The machine system for this method is, as shown in Fig. 1, consists of a small-sized driving
100 machine, a conveying pump, a mixing plant for producing the fluidized sand, and a backhoe for
101 supplying sand in the hopper. The machine system occupies a small area of about 3 m by 6 m.
102 In the mixing plant, the fluidized sand is produced by mixing water, fluidizing reagent and
103 retarding plasticizer with sand, and then transferred to the execution machine by a
104 piston/cylinder type pump to the maximum distance of about 100 m.

105 Figure 4 shows the construction procedure, which is similar manner. The steps from (1) to (4)
106 can perform the same quality of compaction as the conventional SCP.

107 (1) After positioning machine, a casing rod is drilled and is installed to design depth.

108 (2) Fluidized sand is discharged from the bottom end of the rod and compressed to
109 manufacture a sand pile of 70 cm in diameter

110 (3) The rod is lifted up the rod about 20 cm for next discharged

111 (4) Repeat step (2) and (3) to design upper level to manufacture compacted sand pile.
112 The fluidizing sand discharged into the ground becomes to granular state gradually by
113 the retarding plasticizer agent.

114 ***2.3 Case history of improvement for existing structures [3]***

115 In this section, one of case histories of the method is briefly introduced where it was
116 applied to improve the seismic behavior of a river dyke close to private houses. Figure 6
117 shows the ground condition at the site and the improvement cross section. This method was
118 selected based on its low noise and vibration during execution for minimizing adverse
119 influence to river back side and its small space occupancy to river front side.

120 Several sand and clay layers are stratified at the site as shown in Fig. 6, whose total thickness
121 is about 15 m and the SPT-*N* values varied 1 to 20 along the depth. The target improvement
122 layers are two alluvial sand layers and a clay layer named AUs, ALs and ALc respectively. In
123 the execution, a small sand fill was constructed temporarily on the house side slope of the
124 river dyke as a platform for the machine. The sand piles were constructed at 3 to 8 rows to

125 form square arrangement of 1.2 to 1.9 m spacing. The piles' length was 2 to 14 m while the
126 drilling length from the dyke crest was 9 to 21 m. The two driving machines were used as
127 shown in Fig. 7, where the fluidized sand was manufactured and supplied from one mixing
128 plant located about 100 m far from the site to avoid adverse noise problem to the houses.

129 Figure 8 shows the distribution of SPT- N values along the depth before and after the
130 improvement. The figure clearly confirms that the SPT- N values of the layers were increased
131 to about 20 which could achieve the design requirement. The figure also shows another
132 SPT- N value for comparison that was measured at the river side of the dyke improved by
133 non-vibratory type of SCP method, SAVE method. The figure shows that almost the same
134 increase in SPT- N value could be achieved by the two types of SCP methods even if the
135 machine of the SAVE-SP method is quite small.

136

137 3. Numerical analyses

138 As mentioned above, the new type of SCP method enables us to improve ground underneath
139 existing structure with any arbitrary shape of the compacted portion. This method encourages
140 finding the most effective shape and location of improvement for seismic stability of
141 superstructure. A series of dynamic finite element analyses was carried out to investigate the
142 effect of the shape and location of improved portion on the ground response and
143 deformation mechanism of embankment and ground.

144 *3.1 Ground condition and analysis model*

145 Two dimensional finite element analyses were conducted under the plain strain condition [4].
146 An embankment on a loose sandy ground is exemplified in the analyses as shown in Fig. 9
147 according to the documents and sources which analyzed the damages of embankments in the
148 2011 Great East Japan Earthquake [5, 6]. The sand layer with a thickness of 7 m at the surface
149 is underlaid by the clay layer with a thickness of 3 m, and the deepest layer is 10 m thick gravel
150 layer. The water level is set at a depth of 0.5 m from ground surface. The configuration of
151 embankment is determined from the design standards [7], where the soil parameters of soil
152 layers are listed in Table 1.

153 For the liquefiable layer (sand layer) and improved zone, the extended sub-loading surface

154 model proposed by Hashiguchi and Chen [8] was adopted to simulate the accumulation of
155 pore water pressure due to the cyclic shearing. Their SPT- N value and fine content (F_c), the
156 density of soil particle (ρ_s) and the permeability (k) were assumed based on those at a certain
157 damaged site and other parameters were assumed by the empirical correlations and the cyclic
158 undrained triaxial tests. Figure 2 shows the liquefaction strength curve of the soils used for
159 the liquefiable layer and improvement zone. The improvement ratio of improvement zone is set
160 to 20 % throughout the analyses.

161 The clay layer and gravel layer modeled by Drucker-Prager model were assumed as a non-
162 liquefiable layer in the analysis, where the accumulation of pore water pressure is not
163 considered. The SPT- N value, the plasticity index (I_p), the density of soil particle (ρ_s),
164 permeability (k), of clay layer were assumed. For the gravel layer, the SPT- N value and
165 density of soil particle (ρ_s), permeability (k), were assumed. Other parameters for these two
166 layers were

167 determined using the empirical correlations.

168 The embankment in a dry condition is simulated by the extended sub-loading surface
169 model proposed by Hashiguchi and Chen model [8] to simulate its dynamic behavior. In
170 the analyses, two types of embankment were simulated to investigate the effect of its
171 density on the dynamic behavior: (a) loosely compacted condition and (b) well compacted
172 condition. The soil parameters of the conditions were the same as the liquefiable layer and the
173 improvement zone respectively.

174 The soils saturated with water are sheared under the undrained condition, i.e., no seepage flow
175 is considered in this analysis. System damping was represented by stiffness proportional
176 damping, and the damping ratio used was 1% in the first mode of free vibration system.
177 Number of node of analysis model is 5,673 and that of the element is 5,460. The boundary
178 conditions of the ground are summarized in Table 2. The side boundaries of analytical domain
179 are distant from the embankment and set to be periodic boundary condition.

180 ***3.2 Input earthquake motion***

181 The dynamic response and deformation behavior of ground is affected by many factors such
182 as the frequency characteristic, the phase or amplitude of earthquake motion. The earthquake

183 motion used in the analysis was shown in Fig. 11, which was measured at the ground surface in
184 the 2008 Iwate-Miyagi Earthquake [9]. The input earthquake motion is applied to the base of
185 model, parallel to the ground surface.

186 **3.3 Analysis cases**

187 Total of 10 cases were analysis changing the ground improvement type and the compaction
188 degree of embankment as shown in Table 3 and Fig. 12: (a) block improvement, (b) side
189 improvement, (c) valleyed improvement and (d) V-shaped improvement, and non-
190 improvement. The block improvement simulates a case where the liquefiable foundation
191 ground right beneath the embankment is improved before the embankment construction (Fig.
192 12(a)). The side improvement is presently the most common improvement case by ordinal SCP
193 method for seismic ground improvement of an existing embankment, where the liquefiable
194 layer beside the embankment is improved instead of beneath the embankment (Fig. 12(b)).
195 The valleyed improvement and V-shaped improvement cases are expected applications for the
196 SAVE-SP method, where the sand piles are driven from the side of embankment at an angle. The
197 valleyed improvement derives the case where the working area is limited (Fig. 12(c)). The V-
198 shaped improvement derives the case of the same size working area as the side improvement
199 case, where the liquefiable layer beneath the embankment is improved in parallelogram (Fig.
200 12(d)).

201 **3.4 Results and discussions**

202 As the detail discussions of the analyses were presented in the literature [10], the analyses in
203 the well compacted cases are briefly discussed in this manuscript.

204 **3.4.1 Excess pore water pressure**

205 The excess pore water pressure time histories in the ground under the embankment (at –
206 2.25 m) are shown in Fig. 13. In the cases of no-improvement and side improvement, the
207 excess pore water pressure increases at first but decreases during shaking, which is
208 sensitively due to the lateral stretching of the foundation ground. This in turn indicates that
209 densification right outside of the embankment is not stiff enough to restrict the lateral
210 displacement in the ground. In the cases of the valleyed improvement and V-shaped
211 improvement, the excess pore water pressure increases and is kept high value during shaking,

212 since they functions to restrict the stretch of the unimproved area under the embankment. This
213 reveals that the effect of the improved zone having high stiffness on the restriction of the
214 deformation of the unimproved ground is variable depend on the shape and location of the
215 improved zone.

216 The excess pore water pressure ratio ($\Delta u/\sigma_{v0}'$) distribution after shaking are shown in Fig.
217 14 for various improvement pattern as well as no-improvement case. The excess pore water
218 pressure ratio reaches 1.0 in the liquefiable layer at the free field, which means that this area
219 is totally liquefied. In the cases of no-improvement and side improvement, it is found that
220 the excess pore water ratio remains relatively small value beneath the embankment. This is
221 due to the lateral stretching mentioned above, which was also confirmed in the centrifuge
222 tests and the numerical analyses [11, 12]. Figure 14(b) clearly shows that the ratio remains
223 quite small value in the improved zone even subjected to shaking, which indicates that
224 liquefaction does not take place there. In the cases of the valleyed improvement and the V-
225 shaped improvement (Figs. 14(d) and (e)), it is found that the ratio increases to 1.0 in the
226 unimproved area beneath the embankment, which indicates liquefaction takes place there.
227 They reveals that it may be difficult to prevent the liquefaction in the unimproved area under
228 the embankment locally even in the valleyed improvement and the V-shaped improvement in
229 the in these improvement cases.

230 **3.4.2 Settlement of embankment**

231 The settlement of the embankment may be caused by several factors as illustrated in Fig. 15,
232 which may be classified into (a) lateral stretching of embankment, (b) volumetric compression
233 of embankment, (c) lateral flow of foundation ground, and (d) volumetric compression of
234 foundation ground [13]. Figure 16 shows these components of the embankment settlement.
235 Since the analysis is conducted under undrained condition, the volumetric compression of the
236 ground should be zero. Figure shows that the settlement component due to the volumetric
237 compression of embankment can be negligible as the embankment is assumed to be well
238 compacted in the analysis. It is found that the settlement of embankment due to the lateral
239 flow of ground is dominant in the all cases except the block improvement. In the case of the
240 block improvement, the settlement due to it is quite small value, about 1/4 of that in no
241 improvement. In the cases of the side, valleyed and V-shaped improvements, the settlement due
242 to it is not so small but becomes to about 3/4 of that in no improvement, which reveals the

243 effectiveness of the improvement beneath the embankment. For the settlement component due
244 to the lateral flow of embankment, any shape of improvement can function to reduce it, which
245 is about 1/2 in irrespective of the shape of improvement. The total settlement of embankment
246 is the smallest, about 30% of the no improvement in the block improvement beneath
247 embankment. Three other improvements also show their effect on reducing the settlement to
248 about 74% of the no improvement.

249 **3.4.3 Horizontal and vertical strain distributions**

250 The effect of geometry of improved zone on the dynamic behavior of ground is discussed
251 by comparing the two improvement cases: the side improvement and the valleyed
252 improvement. Figure 17 shows the horizontal and vertical strain distributions along the center
253 line of embankment for various stages, where the compression strain is represented in
254 positive value. According to Fig. 11, the 5, 15, 25 and 50 sec. in the figure correspond to
255 the initial stage of main shaking, at the immediate end of large shaking, at the end of main
256 shaking and at the end of calculation, respectively.

257 In the case of the side improvement (Fig. 17(a)), relatively large horizontal tensile strain occurs
258 in the deep portion of ground, about -7 to -5 m from the ground surface at the initial and soon
259 after the main shaking. These behaviors correspond to the horizontal displacement in the
260 deep portion of ground as shown in Fig. 8. It is found that the horizontal tensile strain also
261 takes place in the embankment. The horizontal tensile strain tends to predominate in the deep
262 portion soon after the large shaking 15 sec. According to the behavior mentioned above, it
263 can be said that not only the whole portion of the embankment but also the deep portion of
264 the ground under the embankment laterally stretch during shaking.

265 In the case of the valleyed improvement, the horizontal tensile strain in the shallow portion of
266 the ground tends to predominate, while that in the embankment tends to decrease as it get
267 closer to the crest. This tendency was also seen in the V-shaped improvement case. Therefore,
268 it can be said that the area around the embankment crest tends to be compressed, while the
269 lower part of the embankment laterally stretches during shaking. This suggests that the
270 valleyed or V-shaped improvement can minimize the serious earthquake-induced cracking at
271 the crest, although the marked advantage cannot be seen in reducing the total settlement.

272

273 4. Concluding remarks

274 In this manuscript, the outline of the new type of SCP method and the numerical analyses
275 were presented to emphasize the effectiveness of improvement underneath existing
276 embankment on liquefaction prevention and stability increase of embankment.

277 The new type SCP method was developed where granular sand is fluidized to inject into the
278 ground and then re-granulated to manufacture compacted sand piles. This method has many
279 advantages such as high applicability to improvement underneath existing structure, low noise
280 and vibration to minimize adverse influence to surrounding. The case history also shows high
281 improvement performance which is almost same as the ordinary SCP method. The numerical
282 analyses were carried out to discuss the effect of improvement underneath the embankment on
283 the liquefac- tion prevention and stability of embankment. The analyses reveal that the
284 improvement underneath the embankment, valleyed and V-shaped improvements, prevents the
285 lateral stretching of the ground beneath embankment which can provide increase of
286 embankment stability and reduction of embankment settlement.

287 Last but not the least, a lot of research efforts and new ground improvement techniques are
288 required to reinforce not only new but also existing structures against anticipated huge
289 earthquakes in future.

290

291 References

- 292 [1] Kitazume M. The Sand Compaction Pile Method, Taylor & Francis, 2005.
- 293 [2] Imai Y, Ohbayashi J, Fukushima S, Itoh T. Improvement effectiveness and application
294 of sand-injection type static compaction method. Proc of the 54th Geotechnical
295 Engineering Symposium. 2009;579-84. (in Japanese).
- 296 [3] Kubo Y, Uno M, Nakade Y, Fukada H, Takeuchi H. Application examples of sand-
297 injection type static compaction method for earthquake- resistant strengthening work in
298 Shonai River. Proc of the 22nd Technical Session on Investigation, Design and
299 Construction of Japanese Geotechnical Engineering in Chubu Region, 2013. (in
300 Japanese).
- 301 [4] Takahashi A. Soil-pile interaction in liquefaction- induced lateral spreading of soils. D.

302 Eng. dissertation, Tokyo Institute of Technology. 2002.

303 [5] Kanto Regional Development Bureau, Ministry of Land, Infrastructure, and Transport.
 304 Analysis on failure mechanism and factor of failure on levees Material-4. 3rd meeting
 305 on investigation of restoration methods of levees in Kanto District. 2011. (in Japanese).

306 [6] Tohoku Regional Development Bureau, Ministry of Land, Infrastructure, and
 307 Transport. Report on restoration methods of levees in Kitakami River. 2011. (in
 308 Japanese).

309 [7] Japan River Association. Government ordinance for structural standard for river
 310 administration facilities. 2008. (in Japanese).

311 [8] Hashiguchi K, Chen Z-P. Elastoplastic constitutive equation of soils with the subloading
 312 surface and the rotational hardening. *International Journal for Numerical and Analytical
 313 Methods in Geomechanics*. 1998;22(3):197-227.

314 [9] National Research Institute for Earth Science and Disaster Prevention. K-NET,
 315 KiK-net. [cited 2013. Aug 17]. Available from: [http://www.kyoshin.bosai.go.jp/cgi-
 316 bin/kyoshin/getdata.cgi?0+IWTH24+KiK-net](http://www.kyoshin.bosai.go.jp/cgi-bin/kyoshin/getdata.cgi?0+IWTH24+KiK-net).

317 [10] Takahashi A, Sato N. Influence of ground improvement geometry on seismic response
 318 of liquefiable ground. *Proc 2014 Taiwan–Japan Symposium on the Advancement of
 319 Urban Earthquake Hazard Mitigation Technology, Jhongli, Taiwan, 2014*;17-20.

320 [11] Koga Y, Matsumoto O. Shaking table tests of embankment resting on liquefiable sandy
 321 ground. *Soils and Foundations*. Japanese Society of Soil Mechanics and Foundation
 322 Engineering. 1990;30(4):162-74.

323 [12] Tobita T, Iai S, Ueda K. Dynamic behavior of embankments resting on liquefiable sandy
 324 deposits. *Proc of the 3rd International Conference on Urban Earthquake Engineering*.
 325 Tokyo, Japan. 2006;113-20.

326 [13] Okamura M, Matsuo O. Effects of remedial measures for mitigating embankment
 327 settlement due to foundation liquefaction, *International Journal on Physical Modelling
 328 in Geotechnics*. 2002;2(2):1-12.

329

330 Table 1 Soil parameters
331

Liquefiable layer and Improved zone (Hashiguchi and Chen model)		
Parameter	Liquefiable layer	Improved zone
κ	0.0013	0.00036
λ	0.0339	0.0198
e_0	0.944	0.729
ν	0.33	0.28
ρ_s (Mg/m ³)	2.7	2.7
ϕ (°)	30.4	37.7
ϕ_d (°)	25	25
μ	1.5	0.4
ϕ_b (°)	20	20
b_r	100	20
u_1	4	2.5
m_1	2	2.5
c	20	3
k (m/s)	5.0×10^{-5}	5.0×10^{-5}
OCR	1.2	4.7
s_{ij0}/σ_{ij0}	0.1	0.01
K_0	0.5	0.4
Clay layer and Gravel layer (Drucker- Prager model)		
Parameter	Clay layer	Gravel layer
E_{98} (N/m ²)	1.38×10^8	3.57×10^9
e_0	1.14	0.45
ϕ	0.33	0.33
ρ_s (Mg/m ³)	2.65	2.70
c (N/m ²)	31300	0
ϕ (°)	0	40
ψ (°)	0	10
k (m/s)	1.0×10^{-8}	5.0×10^{-5}

332
333 Table 2 Boundary conditions
334

Name	Initial stress analysis		Dynamic analysis	
	X	Y	X	Y
A	Fix	Free	Periodic	Free
B	Periodic	Free	Periodic	Free
C	Fix	Fix	Fix	Fix
Other nodes	Free	Free	Free	Free

335
336

337 Table 3 Analysis cases

338

No	Name	Improvement type	Embankment
1	IM0L	No improvement	Loosely compacted
2	IM1L	Block improvement	
3	IM2L	Side improvement	
4	IM3L	Valleyed improvement	
5	IM4L	V-shaped improvement	
6	IM0W	No improvement	Well compacted
7	IM1W	Block improvement	
8	IM2W	Side improvement	
9	IM3W	Valleyed improvement	
10	IM4W	V-shaped improvement	

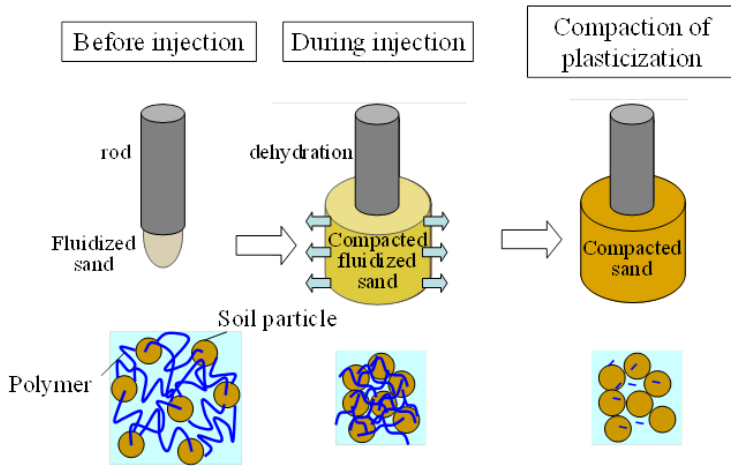
339



340 View of execution system

341 Fig. 1 SAVE-SP machine and mixing plant.

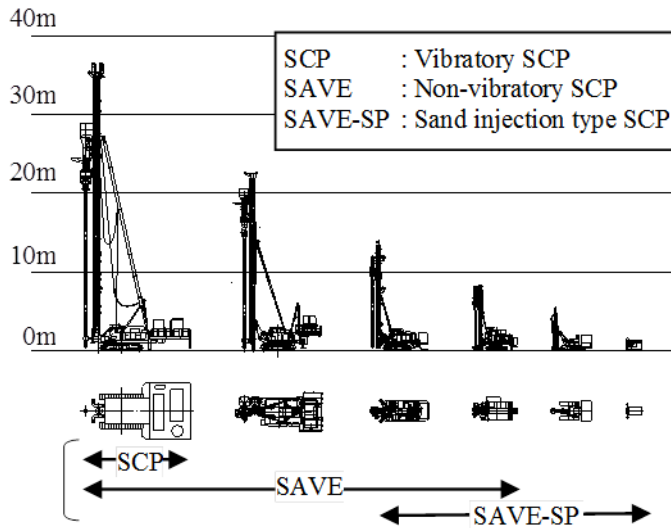
342



343

344 Fig. 2 Schematic view of mechanism of the method.

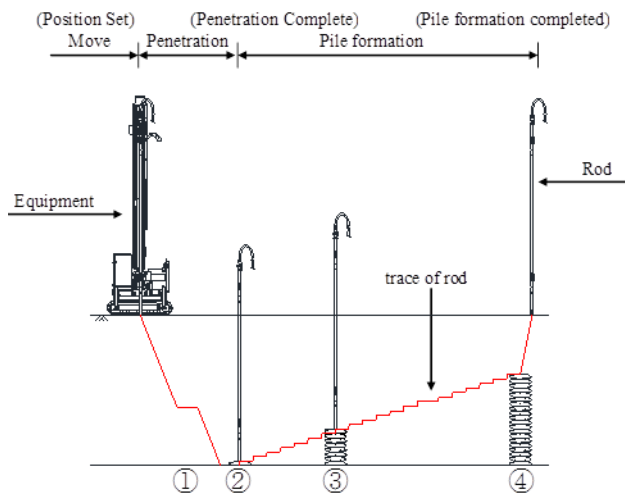
345



346

347 Fig. 3 Comparison in execution machine scale.

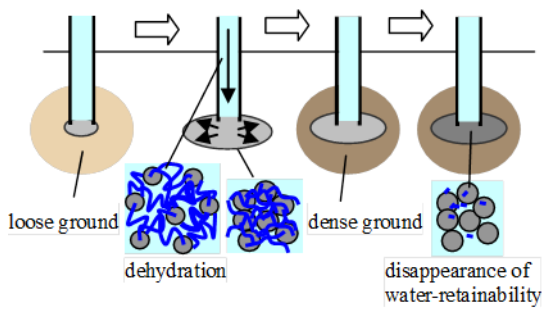
348



349

350 Fig. 4 Process for implementation

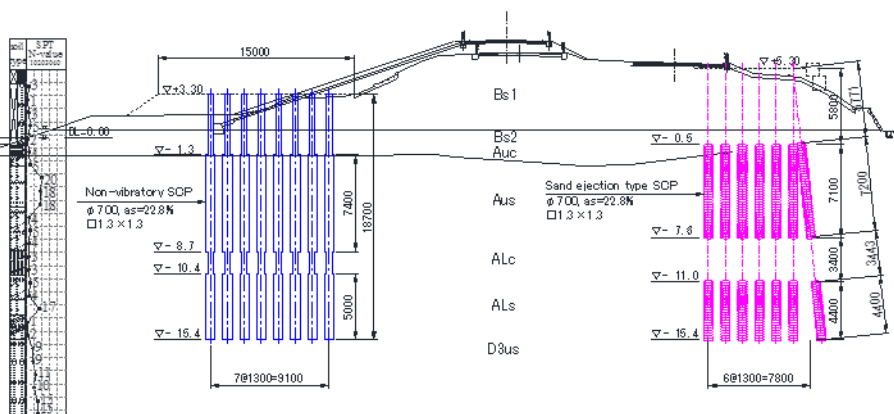
351



352

353 Fig. 5 Mechanism for compaction

354



355

356 Fig. 6 Cross section and soil condition of the site and arrangement of sand piles

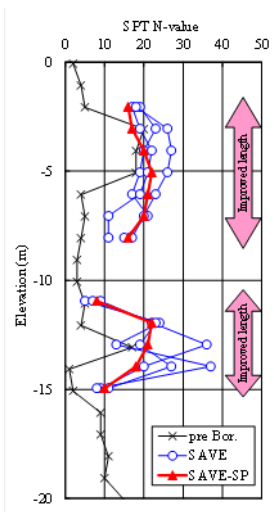
357



358

359 Fig. 7 Machines working at state

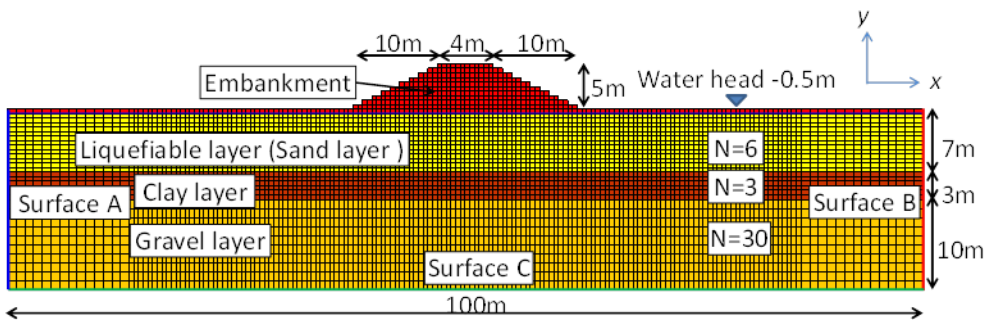
360



361

362 Fig. 8 SPT-N value distributions before and after improvement

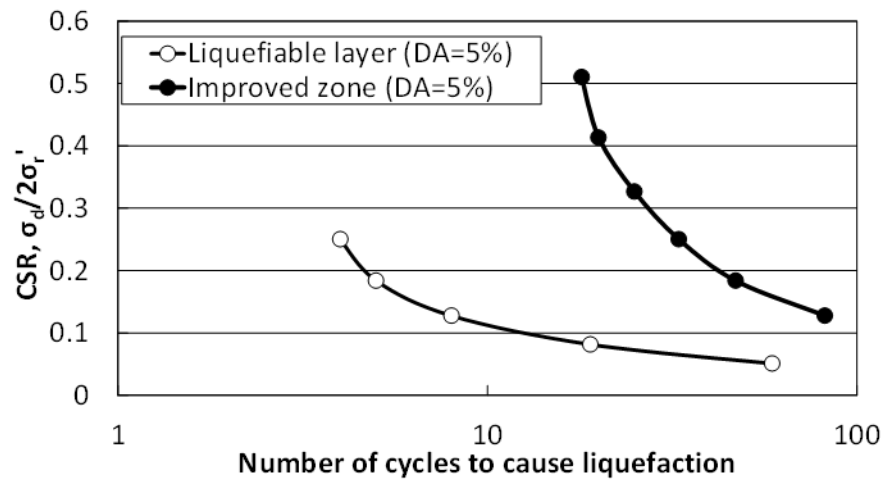
363



364

365 Fig. 9 Model ground analyzed

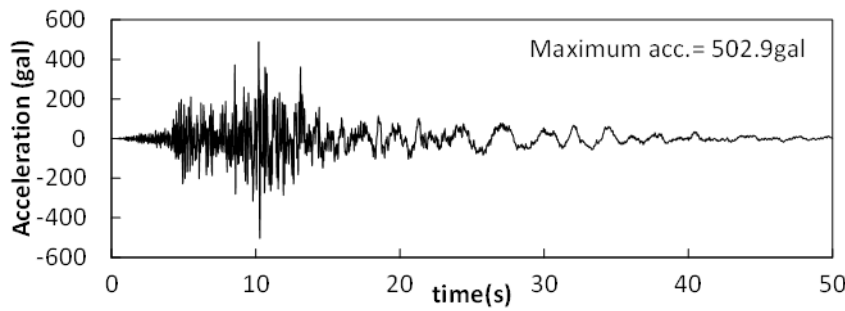
366



367

368 Fig. 10 Relation between cyclic stress ratio and number of cycles to cause liquefaction

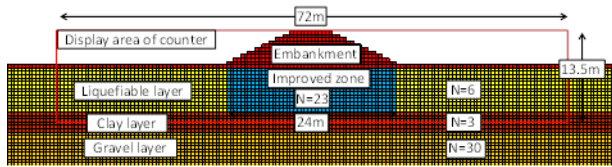
369



370

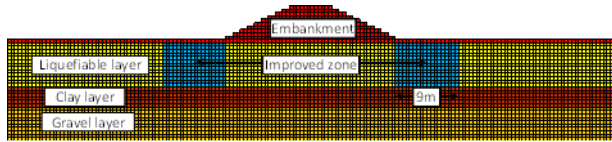
371 Fig. 11 Input earthquake motion (2003 Iwate-Miyagi Earthquake[8])

372



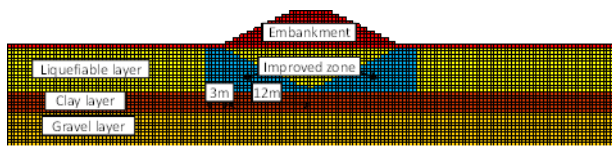
373

(a) Block improvement (IM1L, IM1W)



375

(b) Side improvement (IM2L, IM2W)



377

(c) Valleyed improvement (IM3L, IM3W)

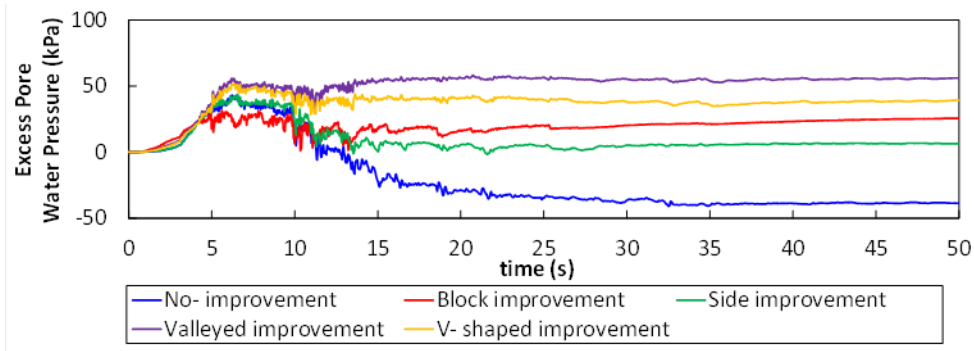


379

(d) V-shaped improvement (IM4L, IM4W)

381 Fig. 12 Analysis cases (improvement condition)

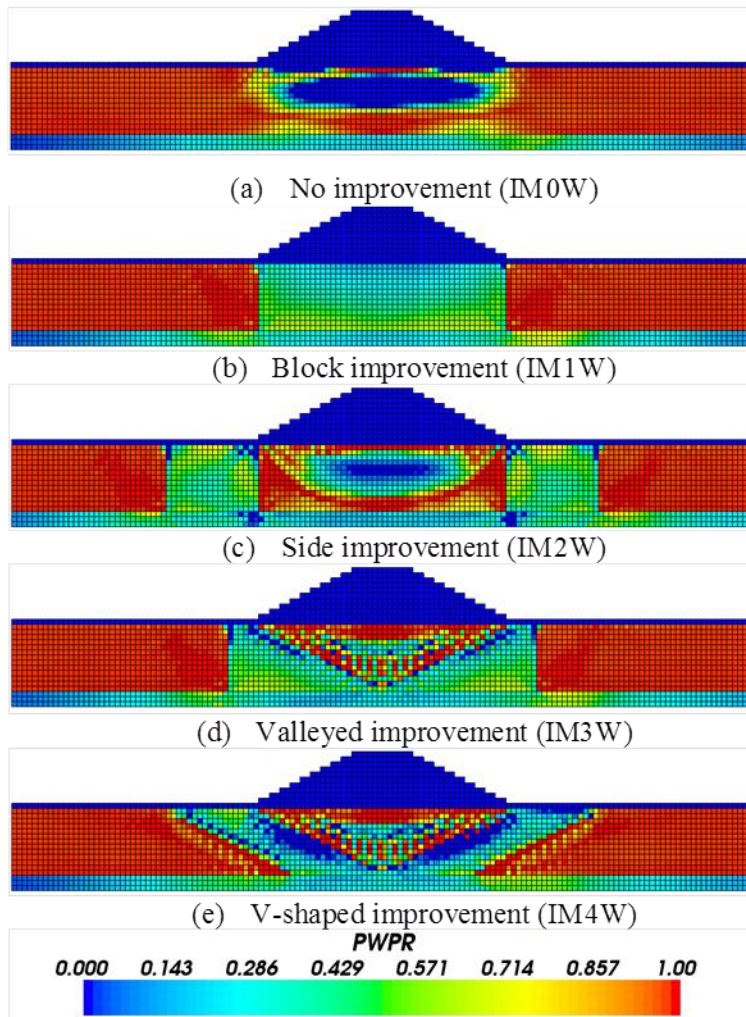
382



383

384 Fig. 13 Excess pore water pressure time history in the foundation ground under the
 385 embankment (-2.25m)

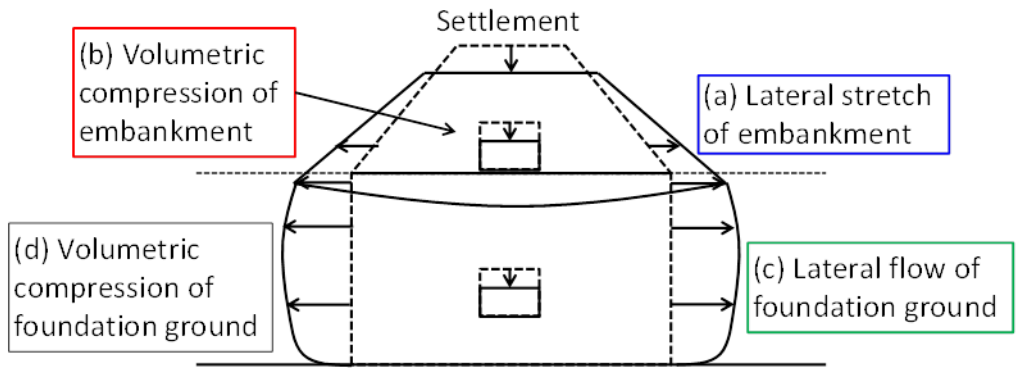
386



387

388 Fig. 14 Excess pore water pressure ratio distribution after shaking (Well compacted cases)

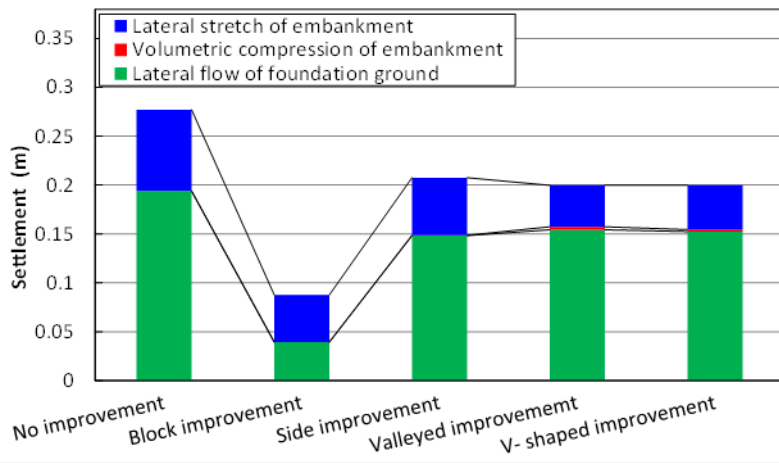
389



390

391 Fig. 15 Primary factors of settlement

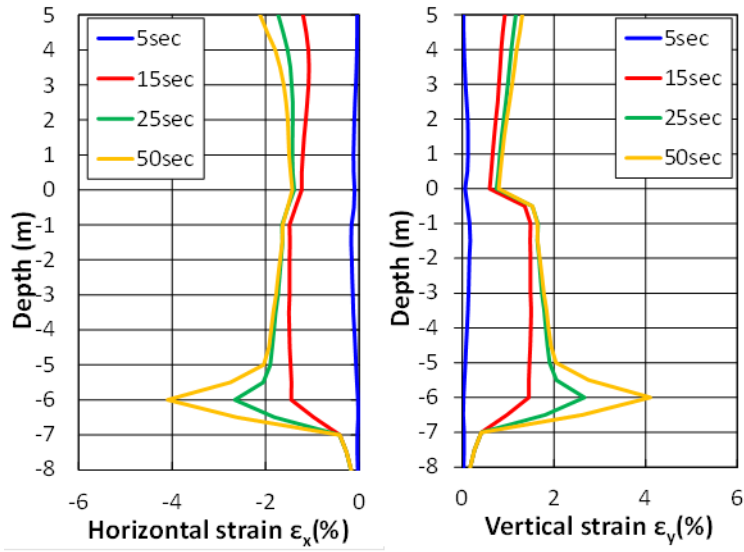
392



393

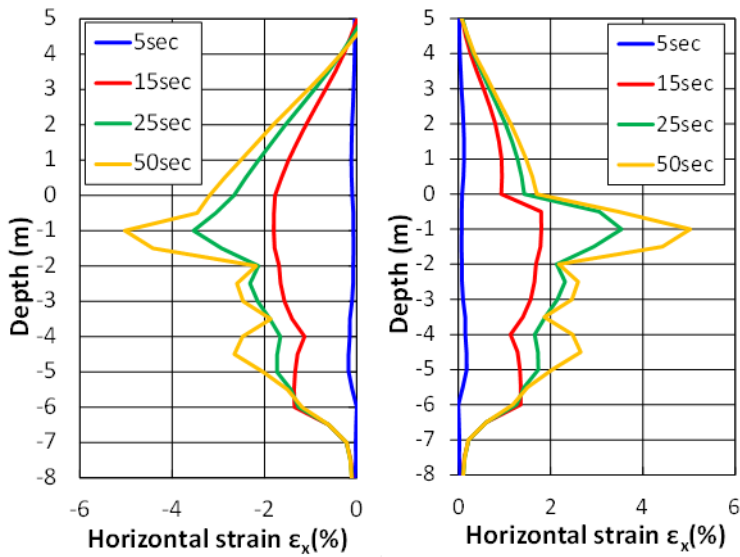
394 Fig. 16 Crest settlement (Well compacted cases)

395



(a) Side improvement (IW2W)

396



(b) Valleyed improvement (IW3W)

397

398 Fig. 17 Horizontal and vertical strain distributions at center of embankment

399